national accelerator laboratory TM-600
1501

SUMMARY REPORT ON PHASE I
OF THE
POPAE DESIGN STUDY
(Part 2)

T.L. Collins, D.A. Edwards, A.G. Ruggiero, L.C. Teng

August 1975

The initial phase of the POPAE Design Study consisted of an investigation of the lattice and layout of the storage rings, and an examination of site factors. Part 1 of the summary report - TM-547 - contained introductory comments and material relating to the proton storage rings. The electron ring and site discussion are the subjects of this Technical Memorandum.

III. The Electron Storage Ring

A. Introduction

Since the proton rings are the primary factor in determining the scale and layout of the facility, comparatively little time was devoted to the electron ring during this phase of the study. As already mentioned in Chapter I, we have examined briefly two versions of the electron storage ring. One of these is the large electron ring proposed at the Aspen Summer Study, to yield a luminosity of $10^{32}cm^{-2}sec^{-1}$ at 20 GeV. The second is a smaller ring, which might be characterized as a 10 GeV machine.

The potential performance of the small ring is naturally less than that of the 20 GeV case. However, we were led to consider it since it offers a more manageable facility and reduces the problem of interference of a third ring with experiments at a crossing of the other two. Possible approaches to the interference problem are outlined in the next section.

So long as unusual values of the crossing insertion parameters are not used, the performance of the two electron rings can be estimated without a detailed design. This we do in Section C. There being no operating experience with electron-proton colliding beam systems, there is probably a greater uncertainty in such estimates than in the case of electron-positron rings.

It is natural to inquire into the suitability of the existing Fermilab synchrotrons as electron injector for the storage ring, and this is the topic of the final section of this chapter.

In keeping with the preceding material in this report, we will assume that the proton beam is unbunched at 400 GeV, with currents of up to 10 amperes. Though we will use the words "electron ring," it is assumed that equivalent performance is desirable for positrons.

B. Location of the Electron Ring

The 20 GeV electron ring would be constructed in the same enclosure as the two proton rings. At the proton-proton interaction regions, the electron ring could be (a) tolerated as a nearby obstruction, (b) temporarily dismantled, or (c) constructed so as to pass some convenient distance away from the p-p crossing. Case (b) certainly precludes simultaneous e-p and p-p running, and because of the long residence period of experimental equipment, will likely mean that either p-p or e-p collisions are studied exclusively for periods measured in years. Case (a) probably rules out simultaneous running, and would make the design of experimental equipment awkward in some cases.

Case (c) is workable but expensive. The bends in the electron ring must be gradual to keep rf power within bounds so a several meter offset in the electron ring has implications for conventional construction. For example, suppose one wishes to offset the electron ring a distance D at a p-p crossing by a combination of S-bends of mean radius R. Then if the radiation loss occasioned by the offset is to be a fraction f of the radiation loss per turn

$$R^3 = \frac{16}{(2\pi)^2} \frac{DR_o^{\,2}}{f^2}$$

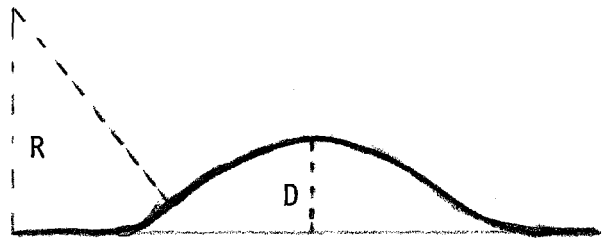

where R_o is the mean radius of the normal curved sectors. For f = 0.1 (a 10% increase in the radiation loss), D = 6 m, and R_o = 936 m, the expression yields R = 597 m! The length of the bypass would be ~239 m.

On the other hand, the version of POPAE considered here contains only one e-p interaction region. A smaller electron ring in its own enclosure avoids the problems of the preceding paragraphs and would lead to a more manageable facility, both from the standpoint of construction and that of operation. Thus we are led to consider a 10 GeV electron ring as an alternative.

Of course, the interference problem still appears at the e-p crossing - now it's one of the proton rings that may be in the way. The same three options, enumerated above as (a), (b), and (c), occur here also, though in (c), one has the constraint that the path difference between the proton rings must be an integral number of wavelengths at the rf injection frequency. As a consequence, if only one beam is deflected in the manner indicated above (with R_0 = 936 m) so as to bypass the e-p crossing, then it is easy to show that the distance between the two proton rings at the interaction is an integral multiple of 42 meters. Since this seems excessive, a less restrictive approach is to cause both proton rings to undergo identical deflections in opposite directions, thereby maintaining the same harmonic number in each. The separation between the proton rings may then be set by the requirements of the e-p experiments.

An example of this procedure for separating the proton rings that is consistent with the lattice described in Chapter II is as follows. Pairs of dipoles 360° apart in betatron phase are combined to deflect the proton rings as sketched below. At the north end, dipoles are inserted in the

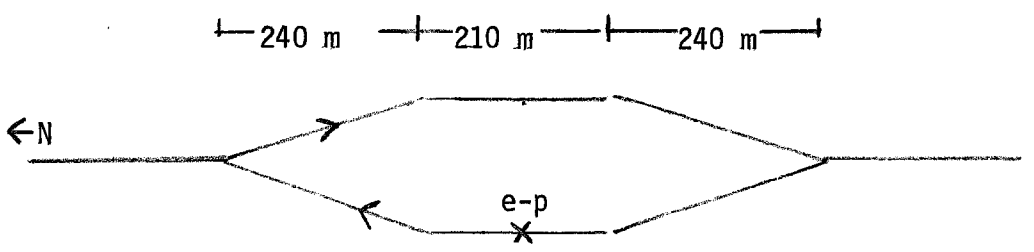

empty half cell which is used to bring the dispersion to zero on entering the east long straight section. The dipoles cause a wave in the dispersion function to propagate into the long straight section, which is removed at the north end of the crossing insertion region by identical dipoles of the opposite sign in field. The high luminosity insertion of Chapter II has a 10.3 m t space at either end which may be used to accommodate the additional magnets. The proton ring which does not intersect the electron ring would not require a special insertion, thus there is no problem in adding the additional dipoles. Similar dipole pairs at the southern end of the insertion region match the dispersion at either end in like fashion. However, in the southern portion of the dog-legs, the region of non-zero dispersion passes through the phase adjusting insertion designated as P_1 in Chapter II. If P_1 is still found to be necessary, it could be moved to the northern end of the west straight section. Assuming that a 13 mrad bend can be placed in the 10.3 m drift in the high luminosity insertion, the separation between proton rings at the e-p intersection would be 6 m.

Throughout this discussion, the presumption has been made that the electron ring will be a third and separate ring. The suggestion is frequently made that one or both of the proton rings be made to serve also for storage of electrons. Though an attractive thought at first glance, severe design problems are implied. Superconducting magnets are already an adequate challenge; to insist that they also provide a magnetic field of suitable quality at 900 gauss (20 GeV) adds yet another constraint. With 5 MW going into synchrotron radiation, the power radiated to the vacuum chamber walls is 1 KW per meter of bending magnet, thus excluding the cold bore possibility.

As will be seen in the next section, the lattice for the electron ring should have a shorter cell length than that of the proton rings. All in all, we do not feel that the combined electron-proton ring presents a realistic alternative at this time.

C. Discussion of Electron Storage Ring Parameters

The purpose of this section is to indicate the performance level that may be anticipated from the two storage ring options. The luminosity of $10^{32}cm^{-2}sec^{-1}$ at 20 GeV set as a goal at the Aspen Summer Study was based on an adventurous set of parameters; here we will follow a more conservative approach in which a more easily realized set of parameters will result in reduced luminosity for initial operation but will allow a subsequent increase in luminosity to the $10^{32}cm^{-2}sec^{-1}$ level by a variety of means that we will outline.

First, we take as the initial limit for power dissipated as synchrotron radiation the figure of 5 MW. A considerably larger figure could be contemplated in the large ring should more rf power prove to be the means of increasing luminosity.

Second, in keeping with the layout of the proton storage rings, we assume that the e-p crossing will be in the vertical plane with the electron ring changing elevation from one side of the crossing point to the other.

Third, the crossing angle will be sufficiently large that the electron beam can avoid nearby elements of the proton ring without the necessity of bending the electron beam in the neighborhood of the intersection point. The rf power requirement for sharp bends is large;[1] however, a possibly more objectionable consequence of a deflection of the electron beam near the crossing is the increased background in experimental equipment arising from synchrotron

radiation. An alternative that deserves exploration is a crossing region wherein the electron ring remains in the horizontal plane, with any change in elevation being performed by the proton storage ring, thereby avoiding any enhancement of the synchrotron radiation background.

Fourth, we will take $\beta_H^* = 1$ meter for both electrons and protons. Smaller values of β^* for the electrons can be considered, but we prefer not to adopt reduced values at the outset in view of the implications for free space about the crossing and for aperture. A crossing angle of 6 mrad will separate the beams by 15 cm at a distance of 25 m - the first quadrupoles of the proton ring can be placed at this distance without excursions in β exceeding those of the insertions of Chapter II, provided a symmetric insertion is used with $\beta_V^* > \beta_H^*$.

Then, provided the emittance of the electron beam is not large compared to that of the 400 GeV proton beam, we need not take into account the variation of beam sizes in the neighborhood of the crossing point in order to estimate the luminosity. The expression analogous to Equation (7) in Chapter II is

$$\mathcal{L} = \left(\frac{2}{\pi}\right)^{1/2} \frac{c\lambda_e\lambda_p}{\left[\sigma_e^{\,2}+\sigma_p^{\,2}\right]^{1/2}\alpha} \tag{1}$$

where λ_e, λ_p are the average linear number densities of electrons and protons respectively, and σ_e, σ_p are the rms (horizontal) beam widths at the (vertical) crossing.

From (1), we see that if σ_e is significantly larger than σ_p the luminosity is diminished, but only limited gain can be made by reducing σ_e below σ_p - a gain at the expense of some concern about the beam-beam tune shift of the protons. To estimate this latter quantity, we will use[2]

$$\Delta\nu_{p,V} = \frac{\lambda_{RF}}{2\pi} \lambda_e \frac{r_p}{\gamma_p} \frac{\beta^*_{p,V}}{(\sigma_{e,H}+\sigma_{e,C})\sigma_{e,C}} \tag{2}$$

$$\Delta\nu_{p,H} = \frac{\lambda_{RF}}{2\pi} \lambda_e \frac{r_p}{\gamma_p} \frac{\beta^*_{p,H}}{(\sigma_{e,H}+\sigma_{e,C})\sigma_{e,H}} \tag{3}$$

$$\sigma_{e,C}^2 \equiv \sigma_{e,V}^2 + \frac{1}{4}\sigma_{e,z}^2\alpha^2 \tag{4}$$

where λ_{RF} is the electron bunch spacing, r_p is the classical radius of the proton, and $\sigma_{e,z}$ is the rms bunch length. For $\sigma_{e,z} = \lambda_{RF}/20$, $\lambda_{RF} = 0.6$ m (500 MHz), $\sigma_{e,H} = \sigma_{e,V} = 0.065$ mm, and an average electron current of 1 ampere, one finds $\Delta\nu_{p,V} = 3.7 \times 10^{-4}\ \beta^*_{p,V}$ and $\Delta\nu_{p,H} = 6.3 \times 10^{-4}\beta^*_{p,H}$. So, even with one ampere of electrons, the proton tune shift is rather small and is not likely to limit the luminosity.

To estimate the tune shift of the electrons due to the proton beam, we can use Equation (9) of Chapter II

$$\Delta\nu_e = \left(\frac{2}{\pi}\right)^{1/2} \frac{r_e}{\gamma_e} \frac{\lambda_p \beta^*_e}{\sigma_{p,H}\alpha} \tag{5}$$

which yields $\Delta\nu_e = 0.03$ for a 10 ampere proton beam having $\sigma_{p,H} = 0.065$ mm intersecting a 20 GeV electron beam at a crossing angle of 6 mrad. Electron-positron storage rings have operated with considerably large values of the parameter $\Delta\nu_e$. For example, the highest value of the linear tune shift reported from SPEAR[3] is 0.08 for each of the two interaction regions, corresponding to $\Delta\nu_e \sim 0.14$ at each intersection.

With the electron and proton beams of comparable size, neither is apparently close to a beam-beam limit. Setting $\sigma_e = \sigma_{p,H}$, the luminosity becomes

$$\mathcal{L} = \frac{c}{\pi^{1/2}} \frac{\lambda_e \lambda_p}{\sigma\alpha} \tag{6}$$

Consider now the two options for the electron storage ring. The larger of the two occupies the same enclosure as the proton rings throughout most of its circumference. The bending radius is therefore 736.2 m, and the energy loss per turn becomes

$$U_o = 1.202 \times 10^{-4} E_{GeV}^4 \text{ MeV/turn} \tag{7}$$

which at 20 GeV is 19.23 MeV/turn. If the radiated power is limited to 5 MW, the electron current is 0.26 amperes. With a proton beam current of 10 amperes, the luminosity from (6) is $4.7 \times 10^{31} cm^{-2} sec^{-1}$, only a factor of two less than the eventual goal. But based on operating experience, a more intelligent judgment can be made than is possible at present as to how the variables of rf power, proton current, crossing angle, and intersection region amplitude functions are to be manipulated to increase the luminosity.

Thus far we have made no statement concerning the lattice of the electron ring, other than that it should follow the proton rings through the semi-circles at either end of the racetrack. The statement that we desire $\sigma_e = \sigma_{p,H}$ at the crossing point implies that the normal cell for the electron ring be about half the length of the normal cell for the proton ring. This may be seen as follows. For a fully coupled electron beam, we have[4]

$$\left(\frac{\sigma^2}{\beta}\right) = \frac{1}{2} C_q \frac{\gamma_e^2}{f_B} \frac{1}{J_H} \frac{1}{\nu_o^3} \left[\left(\frac{\mu_o/2}{\sin(\mu_o/2)} \right)^3 \frac{1 + 3\cos^2(\mu_o/2)}{4\cos(\mu_o/2)} \right] \tag{8}$$

where $C_q = 3.84 \times 10^{-3}$ meters, $J_H = 1$ is the partition number[5] for the

radial betatron oscillations in a separated function lattice, μ_0 is the phase advance in a normal cell, $\nu_0 = N\mu_0/2\pi$ is that part of the tune that is developed in the N normal bending cells, and f_B is the fraction of the normal cell occupied by bending magnets. In writing (8), it is assumed that the effect on (σ^2/B) of cells making transitions from the normal lattice to the insertions is negligible. The arcs at either end of the proton storage rings contain 103 normal cells with a phase advance of 90^0 per cell. Duplication of this structure in the electron storage ring would yield, according to (8), $\sigma^2/\beta = 2.8 \times 10^{-8}$ m for a typical packing factor, f_B, of 0.75. This is about a factor of 7 larger than the 4.2×10^{-9} m desired. A reduction of the cell length by a factor of two will yield a factor of 8 at 90^0 phase advance per cell; 80^0 will produce the factor of 7.

As the electron energy is raised above 20 GeV, the luminosity will vary as E^{-4} provided the electron beam size can be restrained from growing. If the phase advance per electron cell is increased to 130^0 at 40 GeV, the luminosity would be about 10% less than that predicted by an E^{-4} dependence, or $2.6 \times 10^{30} cm^{-2} sec^{-1}$. Beyond this point, the electron beam size will vary directly as the energy, and an E^{-5} dependence of luminosity with electron energy will ensue.

As the electron energy is reduced, the E^{-4} variation is maintained by raising the electron current as E^{-4} and dropping the tune of the electron ring to maintain the beam size. How far one can proceed in this direction depends on one's optimism concerning the electron current that can be stored, for this prescription calls for $2^4 \times 0.26 \cong 4$ amperes at 10 GeV. Average currents up to 1 ampere have been achieved in DORIS;[6] if we use this value as an arbitrary limit, a luminosity of $1.8 \times 10^{32} cm^{-2} sec^{-1}$ is reached at

14.36 GeV below which the luminosity is independent of energy until the electron tune shift limit is reached below 10 GeV.

From 10 GeV to 40 GeV electron energy, the phase advance in the normal electron cell changes from 50^0 to 130^0. The maximum value of the normal cell amplitude function in this range is 75 m. If we say that the vertical aperture should be $20\sigma + 2$ cm, the criterion used in the PEP proposal,[7] then the vertical aperture requirement is 3.1 cm.

Let us turn now to the small electron ring. It is characterized as a 10 GeV ring simply because we require that the same luminosity as that of the larger ring at 10 GeV be achieved in the smaller ring, with the same synchrotron radiation loss and beam current - 1 ampere. The radiation loss per turn is then 5 MeV, implying a radius of curvature in the bending magnets of 177 m. With a packing factor, f_B, of 0.75, the mean radius of the arcs is 236 m. The desire that the fully coupled β of the electron beam be the same as that of the proton beam, 0.065 mm then implies, using (8), that $\nu_0 = 30$. Then the arcs of the racetrack shape electron ring may be composed of a total of 120 cells of 12.4 m in length. Following the E^{-4} dependence, at 20 GeV the luminosity would become $1.1 \times 10^{31} cm^{-2} sec^{-1}$, with the same intersection region parameters as those assumed for the larger ring. Since the amplitude functions scale as the cell length, the vertical aperture required in the normal cells of the small ring would be only 2.7 cm, if we use the same criterion as that employed for the 20 GeV ring.

To summarize, the larger ring offers significant advantages for potential performance. With relatively conservative interaction region parameters, the luminosity would be $\sim 5 \times 10^{31} cm^{-2} sec^{-1}$ at 20 GeV and there are a variety

of steps available to increase that figure, including the straightforward addition of more radiofrequency power. In the smaller ring, the energy deposition per unit length is already very high, and it is unlikely that substantial increase in rf power will be feasible. To raise its luminosity above ~2 x $10^{32}cm^{-2}sec^{-1}$ at 10 GeV requires higher beam currents or a reduced crossing angle. However, the important feature of the smaller ring is the degree to which its construction, operation and maintenance can be decoupled from that of the proton rings. Its adoption would localize the interference problem of three rings to one area and would be a major step toward permitting simultaneous e-p and p-p studies.

D. The Booster and Main Ring as Electron Synchrotrons

Fermilab has, at present, the CEA electron linac in storage. In principle, then, a source of high energy electrons could be obtained relatively quickly and cheaply for initial operation of the electron storage ring by using the CEA linac as the injector into the existing booster. It is most unlikely that this arrangement would be other than an interim measure, and it is examined here on that basis - in particular, we assume that no substantial modifications are made to the booster and main ring to adapt them for use with electrons.

The booster is a 15 Hz combined function machine having unequal radii of curvature and gradients in the focusing and defocusing magnets. Using the following parameters for the booster:[8]

Magnet	B'/B (m^{-1})	ℓ(m)	ρ(m)
F	2.204	2.92	41.21
D	-2.767	2.92	48.49

the partition numbers are $J_H = -2$, $J_E = 5$, $J_V = 1$. Thus, the horizontal

betatron oscillations will have a time constant for anti-damping half that of the conventional combined function synchrotron. The radiation loss per turn is

$$U_0 = 2.00 \times 10^{-3}\ E_{GeV}^4\ \text{MeV/turn} \tag{9}$$

and the characteristic time for radiation damping effects becomes

$$\tau_0 \equiv \frac{E}{\langle P_\gamma \rangle} = \frac{0.787}{E_{GeV}^3}\ \text{sec} \tag{10}$$

With $J_H = -2$, τ_0 is also the e-folding time for horizontal betatron oscillations.

The booster rf system is capable of ~0.7 MV. From (9), the peak electron energy is therefore limited to about 4 GeV, at which $\tau_0 = 12.3$ msec. If acceleration is carried out to the peak of the booster cycle, it is to be anticipated that anti-damping of the horizontal betatron oscillations will have a significant effect on the beam size. Indeed, assuming injection at 250 MeV with $\sigma_H^2/\beta = 0.25$ mm mrad, we find by numerical integration that $\sigma_H^2/\beta = 0.37$ mm mrad for 4 GeV at the peak of the cycle, three quarters of which arises from the radiation excitation term. Reduction of the peak energy to 3.5 GeV yields $\sigma_H^2/\beta = 0.17$ mm mrad.

These emittances are uncomfortably large for the main accelerator as it operates at present. Currently, with injection into the main ring at 8 GeV, corresponding to a guide field of 400 gauss, the figure of 0.17 mm mrad is tolerable. Coupling in the main ring can be used to advantage to reduce σ_H. Injection at 3.5 GeV implies a guide field of ~160 gauss - how the main accelerator would perform at this low field is unknown.

The energy spread out of the booster, on the other hand, is reasonably small. At 4 GeV, $\sigma_E/E = 3.4 \times 10^{-4}$, only about 10% of which reflects the initial energy spread from the linac. In fact, at 4 GeV, σ_E/E is near equilibrium, as the time constant of 5 msec would suggest.

The separated function main ring will have the partition numbers $J_H = J_V = 1$, $J_E = 2$. The time constants for radiation processes will be long, because now

$$U_o = 1.18 \times 10^{-4} E_{GeV}^4 \text{ MeV/turn} \tag{11}$$

and

$$\tau_o = \frac{177}{E_{GeV}^3} \text{ sec} \tag{12}$$

At 4 GeV, the time constant for damping of horizontal betatron oscillations is 5.5 seconds, thus the emittance will change little during the injection dwell time.

Strictly speaking, the main ring ramp rate need not be a constant; however, unless unusual power supply manipulations are performed, it will be a constant over our time scale of interest. Using 3 MeV as the maximum energy delivered to the electrons per turn, acceleration to 10 GeV could be carried out at a ramp rate of 87 GeV/sec, or to 12 GeV at 26 GeV/sec. With the initial conditon of a fully coupled 3.5 GeV beam then $\sigma^2/\beta = 0.030$ mm mrad at 10 GeV or 0.018 mm mrad at 12 GeV. Though these emittances are large compared to the 4×10^{-3} mm mrad on which the electron storage ring apertures were based, those apertures contained a 2 cm allowance for closed orbit excursions, so losses in the storage rings will not likely be excessive.

If 10 ma is delivered by the main accelerator per cycle, 0.25 amperes could be stored in the large electron ring in 34 cycles, requiring a total of just under one minute in the 12 GeV case. The storage of positrons is clearly impractical. This latter circumstance, combined with the operational interference implied by frequent conversion to the acceleration of electrons, is the origin of our feeling that the use of the existing synchrotrons as electron machines can be no more than a temporary expedient.

We conclude that a rapid cycling 10-12 GeV electron synchrotron for use as the electron-positron injector will be required if a serious program of electron-proton colliding beam physics is to be pursued.

IV. SITE CONDITIONS

A. Introduction

As facilities for high energy particle physics have grown to the scale of geographical features of the landscape, so have site conditions become more important cost and performance factors. Enclosures must offer stable support to miles of beam transport systems, access from the surface must be rapid and convenient, a drainage plan is necessary for water level control over an area some square miles in extent, the extensive earthwork needed for radiation safety should not impose excessive off-site requirements for materials, and so on. That the main accelerator enclosure was built quickly and economically is due in no small measure to a siting consistent with a low cost foundation design and straightforward construction techniques.

Viewed in plan, POPAE fits remarkably well on the site. That this is so is partly fortuitous, for there is very little latitude for adjustment, due to the injection requirements. The situation is somewhat less attractive when viewed in elevation, however, and the main topic of this chapter is an examination of topographic and subsurface conditions influencing the elevation of the storage rings.

After the Fermilab site was selected in 1966, 67 widely distributed test borings were drilled by the U.S. Army Corps of Engineers during the period January through September of 1967. Analyses of core samples were carried out to determine engineering properties.[1] The Illinois State Geological Survey developed the pattern and history of the subsurface stratigraphy.[2] Much of the discussion of the next section is based on this site-wide study.

During 1968, numerous additional borings were made by Soil Testing Services, Inc., of Northbrook, Illinois, primarily at locations selected for the principal laboratory facilities.[3] When combined with the Corps of Engineers data, a rather detailed picture of subsurface conditions along the perimeter of the main ring enclosure is obtained. Predictions of enclosure settlement were based on this information, and it is interesting to compare the measured subsidence with the predictions; this we do in Section C. Finally, in Section D we summarize such of the data as is applicable to POPAE and comment on alternatives in elevation and construction technique.

B. Topographic and Subsurface Features

Like most of the surrounding several hundred thousand square miles of the Central Lowlands, the Fermilab site is rather flat - maximum relief over the 6800 acres is only about 70 feet. Along the western boundary, a gentle rise of some 40 feet marks the Minooka Moraine, one of a number of terminal moraines which are roughly concentric with the lower end of Lake Michigan. Just to the east of the site, the Valparaiso Moraine defines a similar line of slightly higher ground. Generally speaking, the lowest surface elevations are to be found in the southeastern portions of the Laboratory, where there are substantial swampy areas. These are drained by Ferry Creek, which crosses the site boundary near the southern end of the east long straight section of POPAE and eventually finds its way to the West Branch of the DuPage River.

The bedrock surface is also relatively flat, decreasing in elevation gradually toward the east, and is encountered typically at depths of between 60 and 100 feet below ground level. This rock is dolomite of the Silurian period. The level of the permanent water table lies within this rock layer,

which is laterally permeable and, according to the Illinois State Water Survey, forms an important aquifer.

The strata between ground surface and bedrock reflect the advance and retreat of "recent" glaciation. Whatever materials overlaid the bedrock in the hundreds of millions of years between Silurian and Pleistocene times have vanished. The glacial deposits have been grouped by the Illinois State Geological Survey into five stratigraphic units, which in descending order are characterized as follows:

Unit A. The surface layer contains silts and sands deposited from lakes or streams, and silts brought in by the wind. The wind-borne materials cover much of the site with a thickness of a few feet, and are mineralogically distinct from the water-deposited materials, which are similar to the underlying strata.

Unit B. This is a glacial till composed primarily of silt and clay, with some sand and gravel. It is much firmer material than Unit A and relatively impenetrable to water. The Minooka Moraine is compared of this till.

Unit C. This layer is a mixture of sand, silt, and gravel. Little clay is present, thus this unit is relatively incompressible.

Unit D. This stratum has the highest clay content (up to 75%) of the various tills. It has higher moisture content and lower density than the till of Unit B. It is possible that this layer is associated with an earlier glaciation than the most recent (Wisconsinan) ice age.

Unit E. This is a sandy and silty till containing deposits of sand and gravel which rests directly on bedrock.

Not all of the above units need necessarily be found in a particular boring, and the strata are by no means as flat as either bedrock or the surface of the ground. Figure 1, taken from reference 2, illustrates the distribution of the various layers along Wilson Road from one site boundary to the other. Note that Unit A is absent in the easternmost portion, near the Minooka Moraine, while both Units D and E vanish in a small region near the center of the Figure.

With the exception of Unit II of the strata have been subjected to glacial overburden and are well consolidated. All of these subsurface layers, if undisturbed, are suitable foundation materials for accelerator enclosures, and so long as the stress which propagates downward from these enclosures, other structures, and shielding does not exceed that imposed by the glaciation, settlement will be within reasonable bounds.

C. The Main Accelerator Enclosure

Design studies of the main accelerator conducted prior to the formation of the Laboratory envisioned that the magnets would be supported on pilings or caissons driven into bedrock. The implications of this approach in cost and complexity are far reaching. The piles themselves are expensive, thus one is lead to arrangements wherein several magnets rest on long girders which are in turn supported by the piles. But then the temperature of the girders must be carefully controlled to minimize expansion and warping; air conditioning for the enclosure is then found to be desirable. The piles themselves should be sheathed in order to protect the load bearing portion from settlement and other motion of the surrounding earth. The more involved the enclosure becomes, the longer the time needed for its construction. And a circumstance that must not be overlooked is that a contractor in preparing

his bid must, out of prudence, add substantial allowances for the delays and uncertainties associated with complex construction.

Thus it is not surprising that the support piles were eliminated from the design at an early stage. That this step could be taken without undue risk was made possible by the understanding of subsurface conditions summarized in the preceding section. With the piles out of the picture, a simple and easily constructed enclosure was feasible.

The tunnel floor elevation of 722.5 feet above mean sea level was high enough to impose no unusual difficulties to a cut-and-fill operation yet low enough so that the foundation material would be that of stratigraphic Unit B. This level was also sufficiently low that subsequent covering of the enclosure by the shielding berm would not create stresses in the subsurface layers exceeding those previously applied by the glacial burden.

The concrete floor of the enclosure rests directly on the till. In those places where unconsolidated materials were found at the base of the cut (for example, a low point in Unit A), they were replaced by lean concrete. Similarly, in the event of over-excavation, lean concrete was used to restore the foundation to the proper level. The enclosure floor was formed and poured in place. The precast concrete hoops (the sides and ceiling of the tunnel) were fabricated on site and placed quickly, yet accurately, on the foundation. The construction sequence therefore consisted of a limited number of steps and proceeded rapidly and smoothly. It should be noted that where more intricate structures were necessary, as in the service buildings, their access-ways to the tunnel, and the transfer hall, these features were slow to complete and disproportionately costly.

How well the elevation chosen for the main ring enclosure conforms with the subsurface conditions is illustrated in Figures 2 and 3. Here, data from the test boring logs has been used to reconstruct the location of the various stratigraphic layers throughout the entire perimeter of the main accelerator. Note that the 722.5 foot elevation indeed lies within Unit B with little exception. Though Unit C is less compressible than B, it not only occurs at too low an elevation for the enclosure, but it rests in turn on the most compressible of the strata, Unit D.

The long term consolidation settlement was predicted[3] to not exceed one inch in all areas and typically considerably less. The maximum differential settlement was also projected to be one inch. It was estimated that 50% of the settlement would have taken place after the elapse of 75 to 150 days following the completion of the berm, and that 90% of the motion would be reached after about 5 to 10 years. The shorter times (and smaller total settlements) are associated with those locations with higher pre-construction surface elevations, hence lesser berm weights.

After the various portions of the enclosure were completed, frequent surveys were conducted to monitor the motion. These surveys were terminated in early 1971 as installation of accelerator components precluded their continuation. As a result, settlement was traced for differing periods depending on location. The data for part of the ring are summarized in Figure 4. Though the settlement estimates were apparently a shade optimistic, the measurements confirm the validity of the foundation concept. The surveys were made under difficult circumstances, and the data are not easy to analyze for motions occurring during a time scale of weeks. It is these motions which

could cause severe interference with accelerator operation due to rapidly changing orbit distortions. A statistical study of the data indicates that had operation of the machine been attempted then, vertical closed orbit distortions of the order of two inches peak to peak would grow in a week or so. A year later, when operation at high energy was achieved, no significant time dependent orbit motion was observed. Since that time, a few quadrupole position adjustments have been made for vertical orbit control - whether or not these have been occasioned by tunnel movements is unclear.

In summary, the design procedure for the main accelerator enclosure has proved to be highly successful, and it is reasonable to expect that a similar approach for POPAE would be no less so, provided that a similar approach can be followed.

D. POPAE

The degree to which the POPAE enclosure may present qualitatively different problems when compared to the main accelerator is suggested by Figure 5 which represents a plot of surface elevation along the perimeter of the proton storage rings. The western half of POPAE passes through regions of surface elevation quite like the main ring situation, as can be seen by comparison with Figures 2 and 3. In contrast, the eastern half of POPAE encounters the low swampy regions on the site. For reference, the main ring tunnel floor elevation is shown in the lower portion of Figure 5.

The borings carried out by the Corps of Engineers included a series along Eola Road, which runs roughly parallel to and about 300 feet to the east of the west long straight section of POPAE. The geologic profile deduced from the set of borings is sketched in Figure 6. Of course, the smoothness

of the strata as compared to Figures 2 and 3 is only a result of the borings being farther apart. It is nevertheless clear that the subsurface conditions for the west half of POPAE do not differ from those for the main ring. Here, one may wish to place the floor of the POPAE enclosure at a slightly higher level than that of the main ring - 730 feet above sea level might be a good choice. This elevation is still consistent with the use of Unit B as the foundation material, and would improve access to interaction regions. The 730 feet choice would also be consistent with drainage requirements. Surface water is presently drained from the area bounded by the main ring berm through a set of pipes passing through the berm and above the tunnel at the eastern edge of the ring. These pipes are at an elevation of 737 feet, and with the bearing level of the POPAE enclosure suggested above, the easterly drainage pattern could be maintained by culverts passing under POPAE.

In contrast, the situation along the eastern edge of POPAE contains a mixture of unknowns and disturbing features. The average surface elevation indicates that a lower elevation of the enclosure floor would be preferable. This in itself is not an insurmountable problem, for a "hinge" can be made at the north and south extremities of the storage rings by interposition in the lattice of vertical bending magnets (in pairs separated by 180° in betatron oscillation phase in order that vertical momentum dispersion be localized) to tip the eastern half downward. Consider two alternative elevations for the east long straight section, with the enclosure floor at 695 feet or at 720 feet.

At 695 feet, the tunnel will be sufficiently low that drainage from the area in the interior of the rings can pass over the enclosure, just as in the case of the main ring. Though subsurface conditions have not been

explored in detail in this portion of the site, indications are that compacted till will still be available for the bearing surface. The disadvantages of this low an elevation are the depth of excavation needed - over 40 feet in some places - and the poor access to experimental areas and to the enclosure that would result. Water would likely pose a greater problem than was the case in the main ring. Dams would be needed inside the rings near the south end of the long straight section to prevent flooding of the excavation.

At a higher level for the enclosure floor - about 720 feet - drainage could be placed under the tunnel. This is a much better elevation for provision of access to the enclosures and experimental areas. However, the quantity of surface and near-surface earthwork implied is enormous. For substantial distances - the greater part of a mile - the tunnel floor would be above present surface level and/or above the upper boundary of compacted till. Large quantities of gravel would be needed from off-site to build up the foundation after removal of the surface soils. This material could be compacted as it is laid down. But it is likely that, in order to avoid excessive settlement after construction, it would be necessary to build up the shielding berm, wait a year or so for the subsurface to adjust to the new loading, and then strip off the berm and construct the enclosure.

Note that in the second case, the beam elevation is above the surface of nearby off-site regions. The massive berm-extensions for muon shielding will create a quite different loading problem than the nearly line-load represented by the main ring.

The very limited test boring information that is available in the neighborhood of the low areas is summarized in Figure 7, where it is seen that though the till layers deform somewhat in the neighborhood of drainages, they

are nevertheless still present. A more detailed field investigation is needed before a serious plan can be developed for the eastern portion of the facility. Nevertheless, it is already clear that construction associated with the eastern half of POPAE will present problems more severe than those for the main accelerator and that higher costs are implied.

REFERENCES

Chapter III

1. M. Tigner, TM-520, September 1974.

2. M. Sands, "The Physics of Electron Storage Rings," SLAC 121, November 1970, page 65.

3. "Measurements on Beam-Beam Interaction at SPEAR," presented by H. Wiedemann, IEEE Transactions on Nuclear Science, Volume NS-20, No. 3, 752 (1973).

4. D. A. Edwards, TM-566, April 1975.

5. Reference 2, page 110.

6. G. Voss, 1975 Particle Accelerator Conference (to be published).

7. J. R. Rees, Proceedings of the IXth International Conference on High Energy Accelerators, SLAC, 1974, page. 564.

8. E. L. Hubbard, et al, TM-405, January 1973.

REFERENCES

Chapter IV

1. Final Report, Preliminary Foundation Analysis for 200 BeV Accelerator, Weston Site Illinois, prepared by Corps of Engineers, Chicago District, December 1967.

2. R. A. Landon and John P. Kempton, Stratigraphy of the Glacial Deposits at the National Accelerator Laboratory Site, Batavia, Illinois, Illinois State Geological Survey, Urbana, Illinois, Circular 456, 1971.

3. Boring Logs and Summary of Related Laboratory Test Data, June 1968. Discussion, Subsurface Investigation, August 1969. Soil Testing Services, Inc., Northbrook, Illinois.

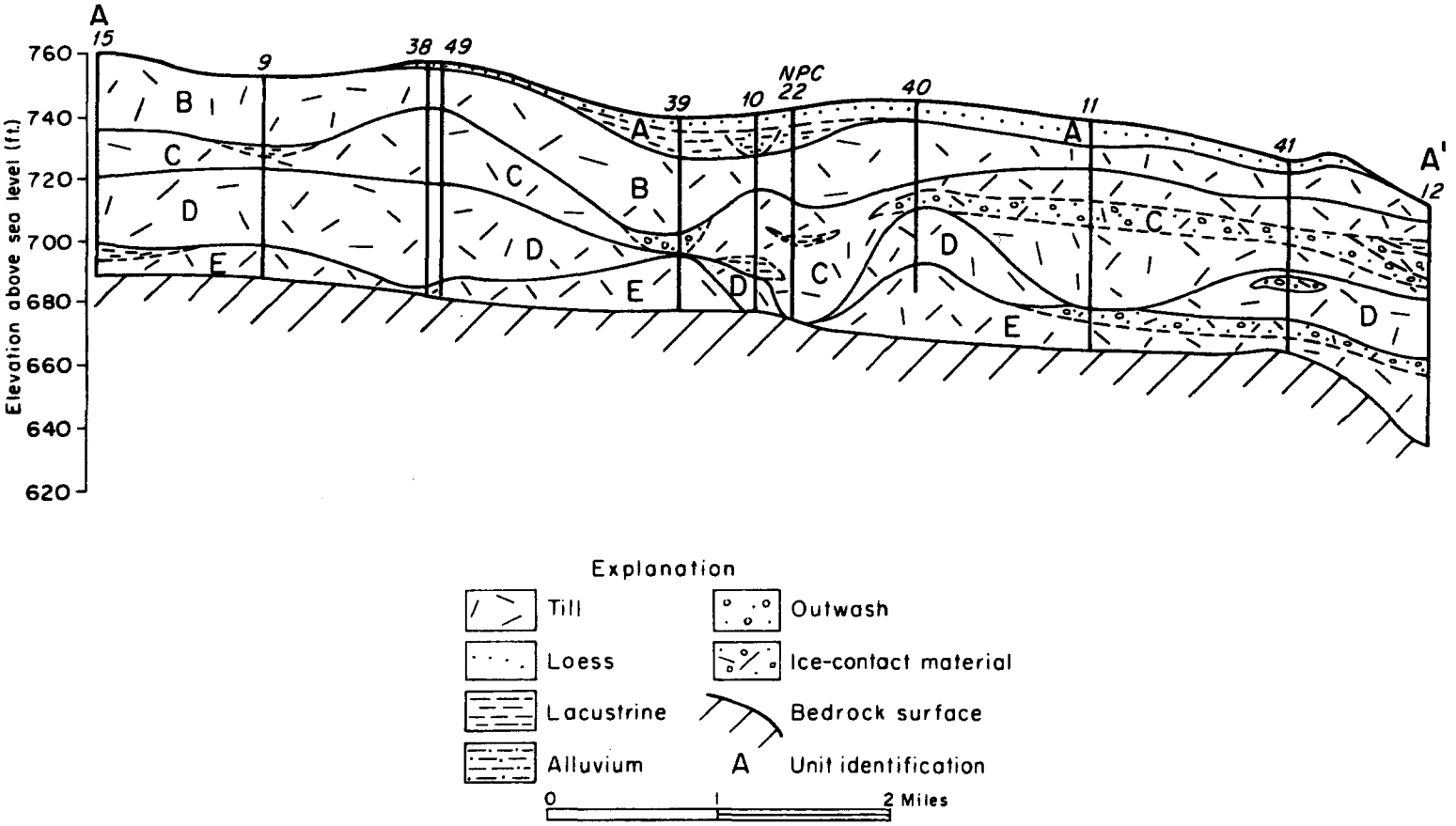

FIG. 1

Geological profile from west site boundary (A) to east site boundary (A') along Wilson Road. Reproduced from Reference 2.

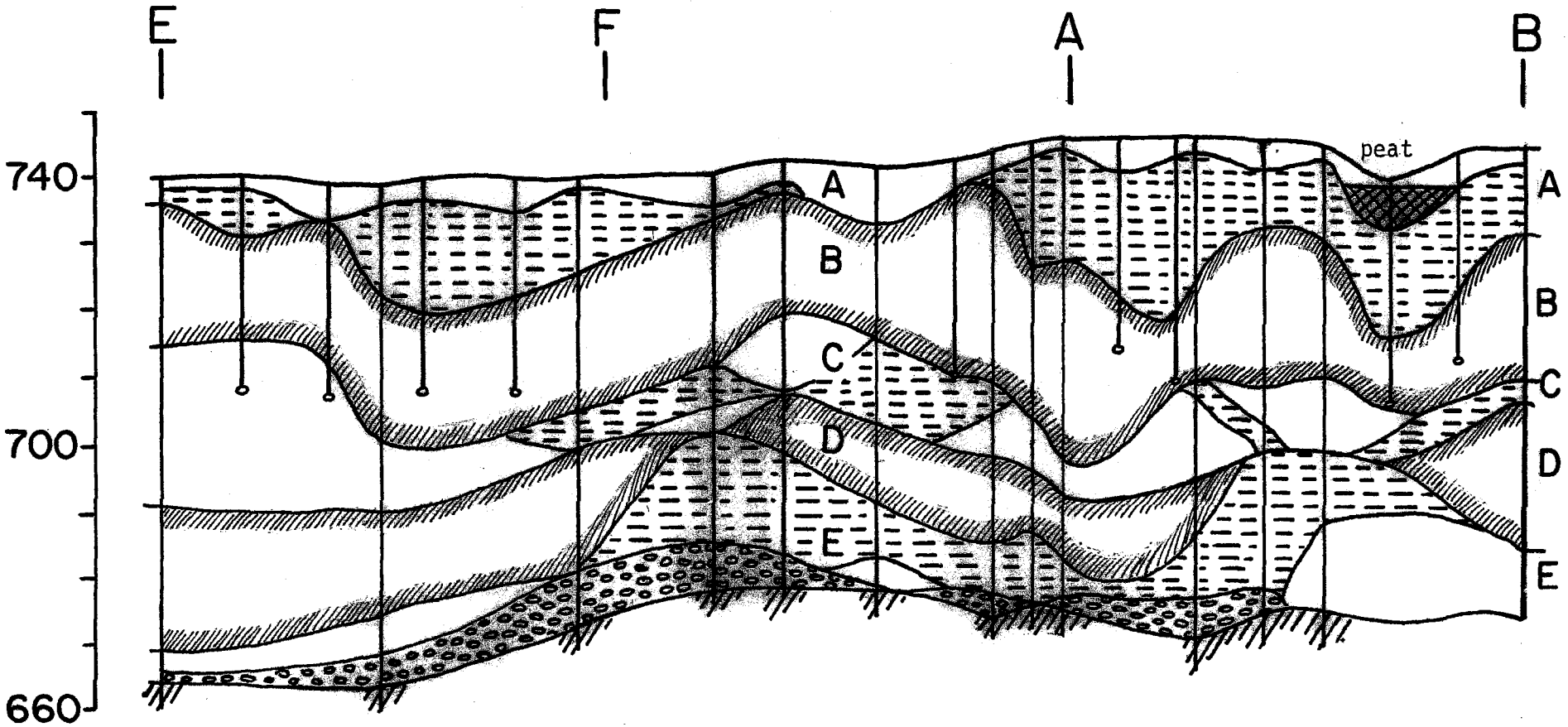

FIG. 2

Geological profile - western half of Main Ring.

TM-0600

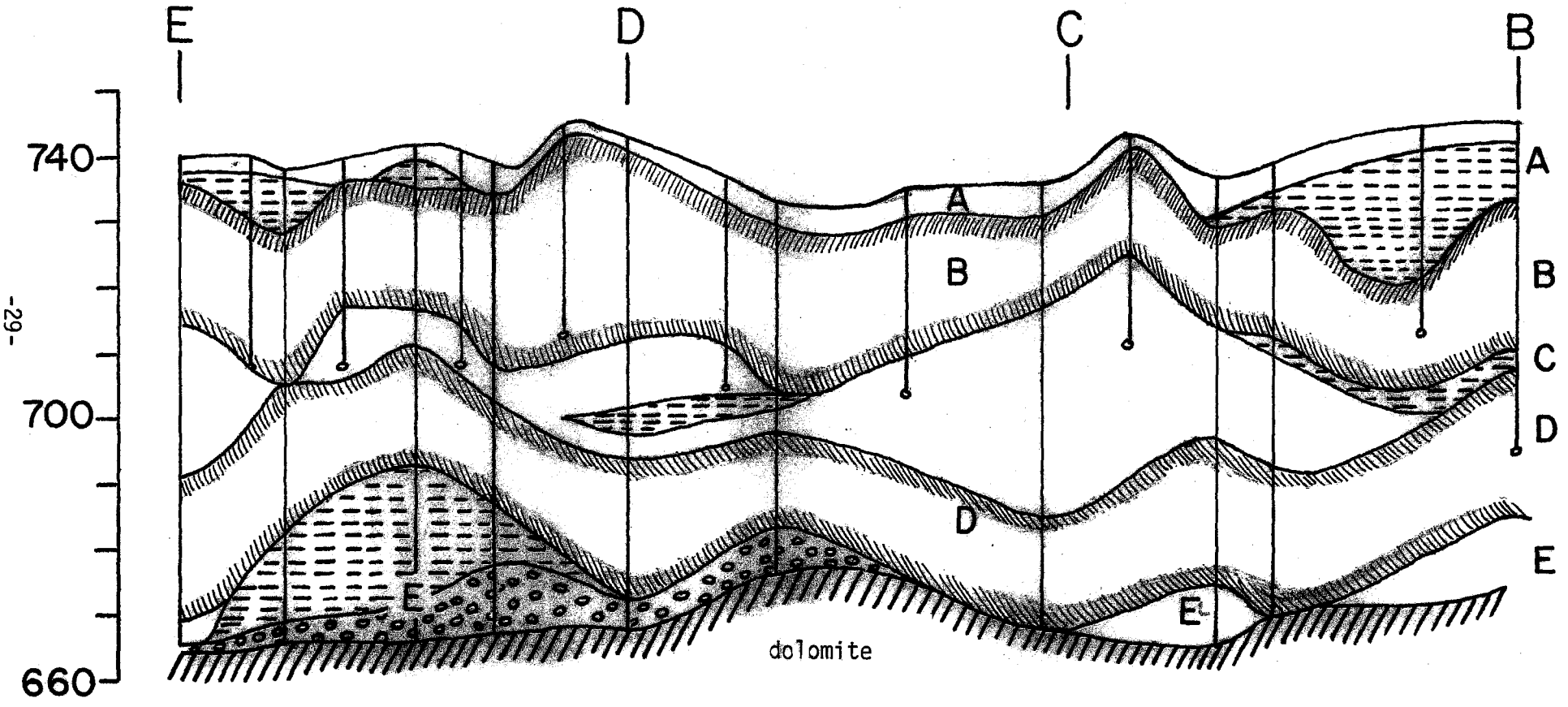

FIG. 3

Geological profile - eastern half of Main Ring.

TM-0600

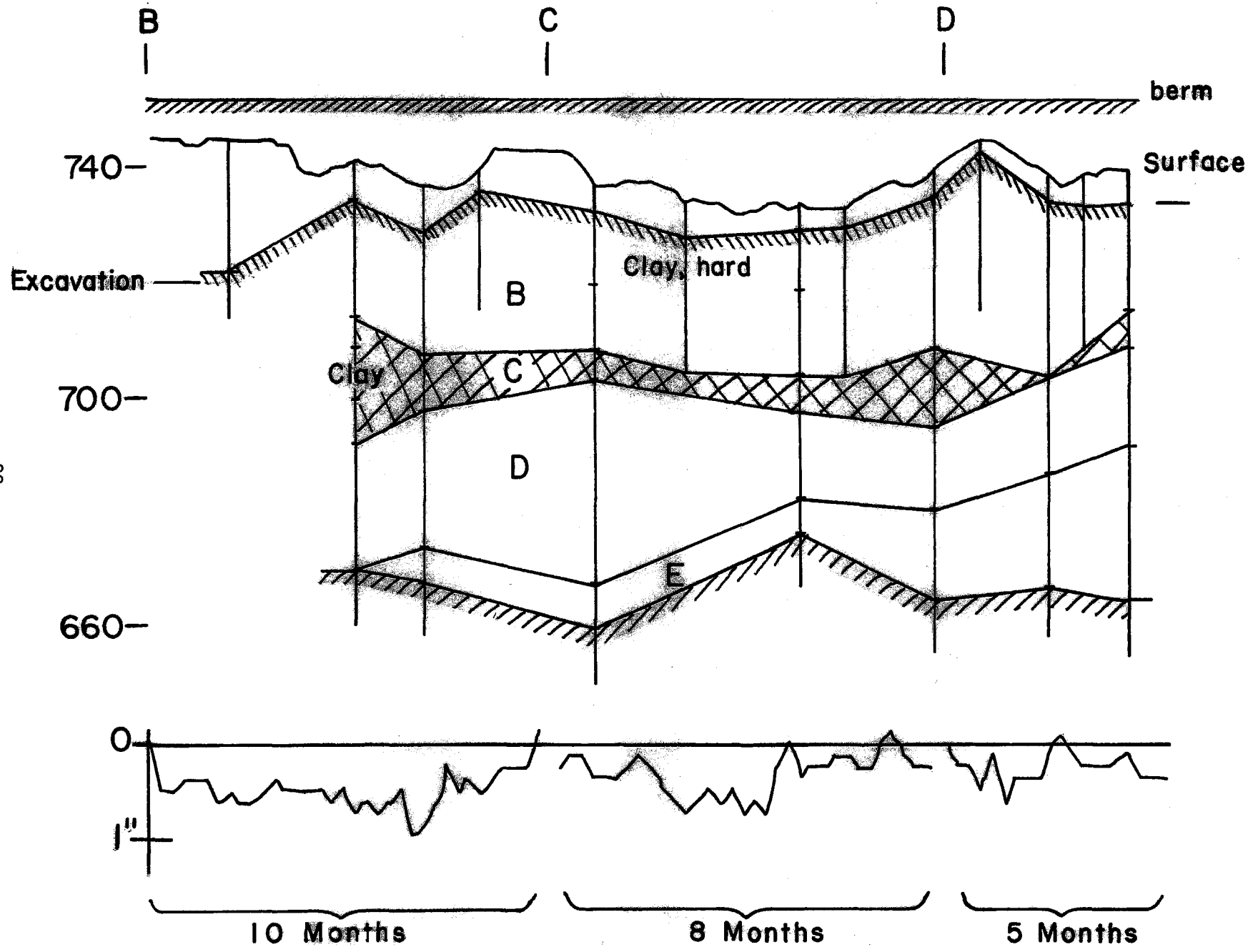

FIG. 4

Post-construction settlement data for portion of Main Ring enclosure.

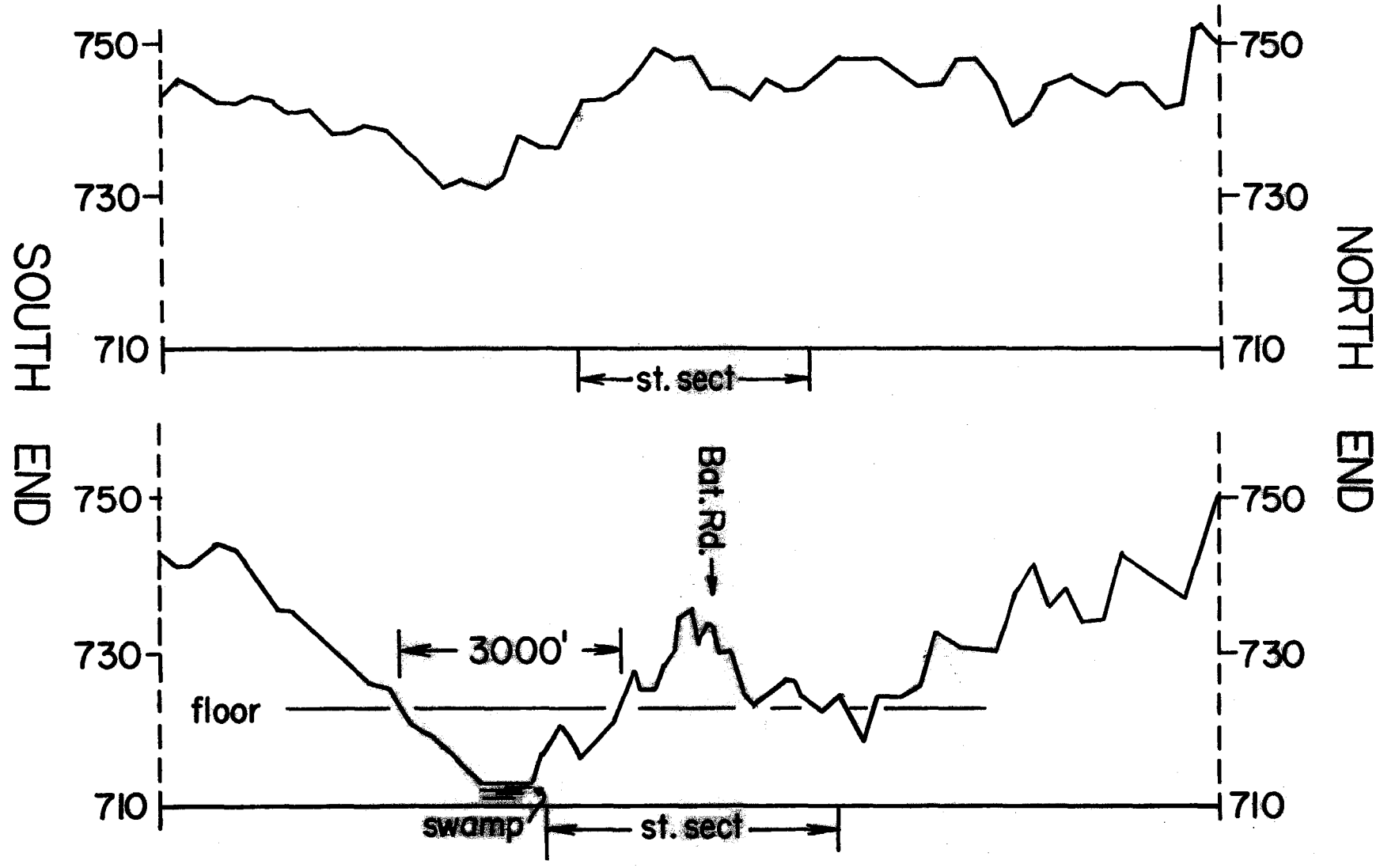

FIG. 5

Surface elevations on perimeter of POPAE.

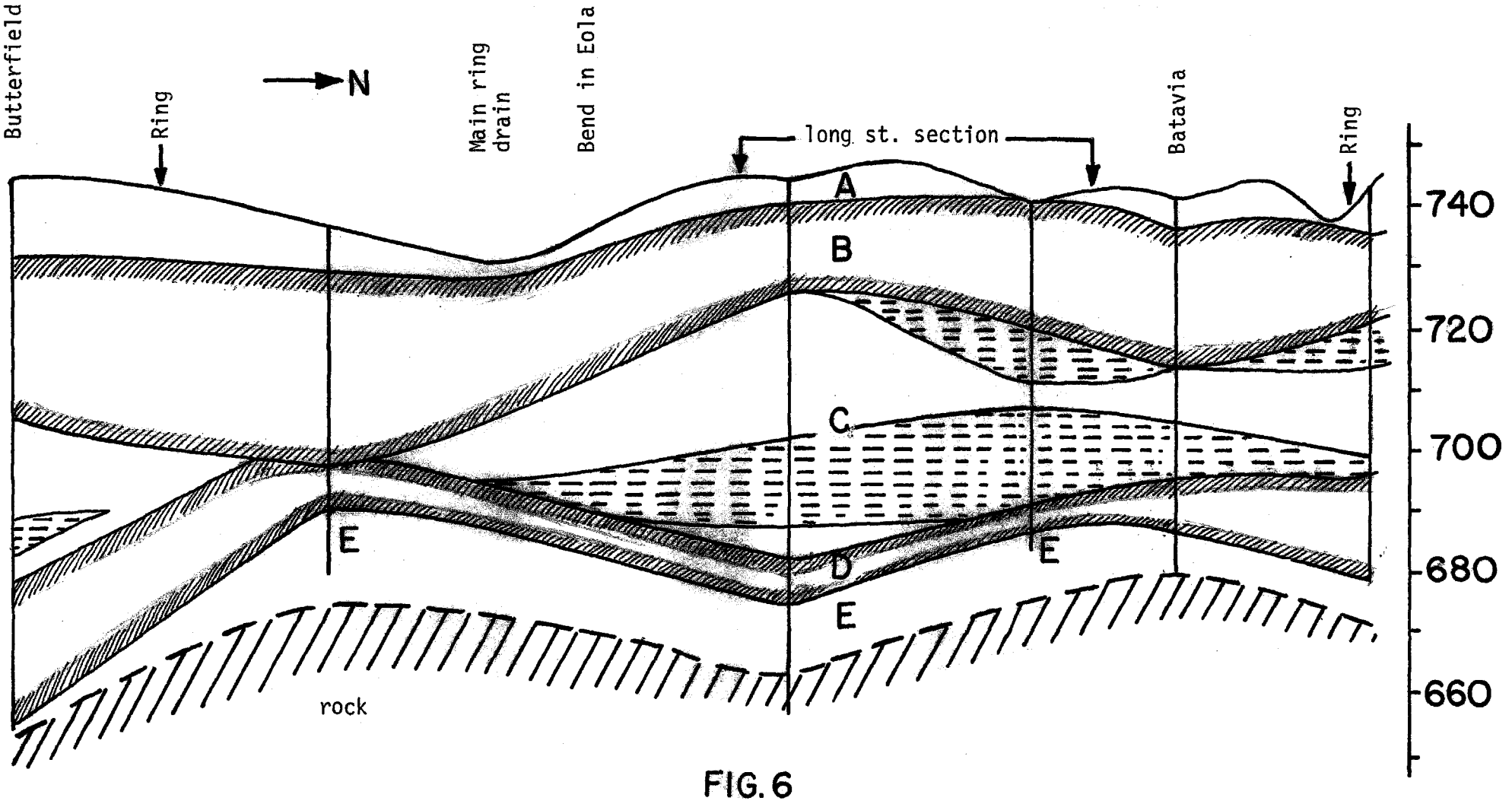

FIG. 6

Geological profile - western side of POPAE (along Eola Road).

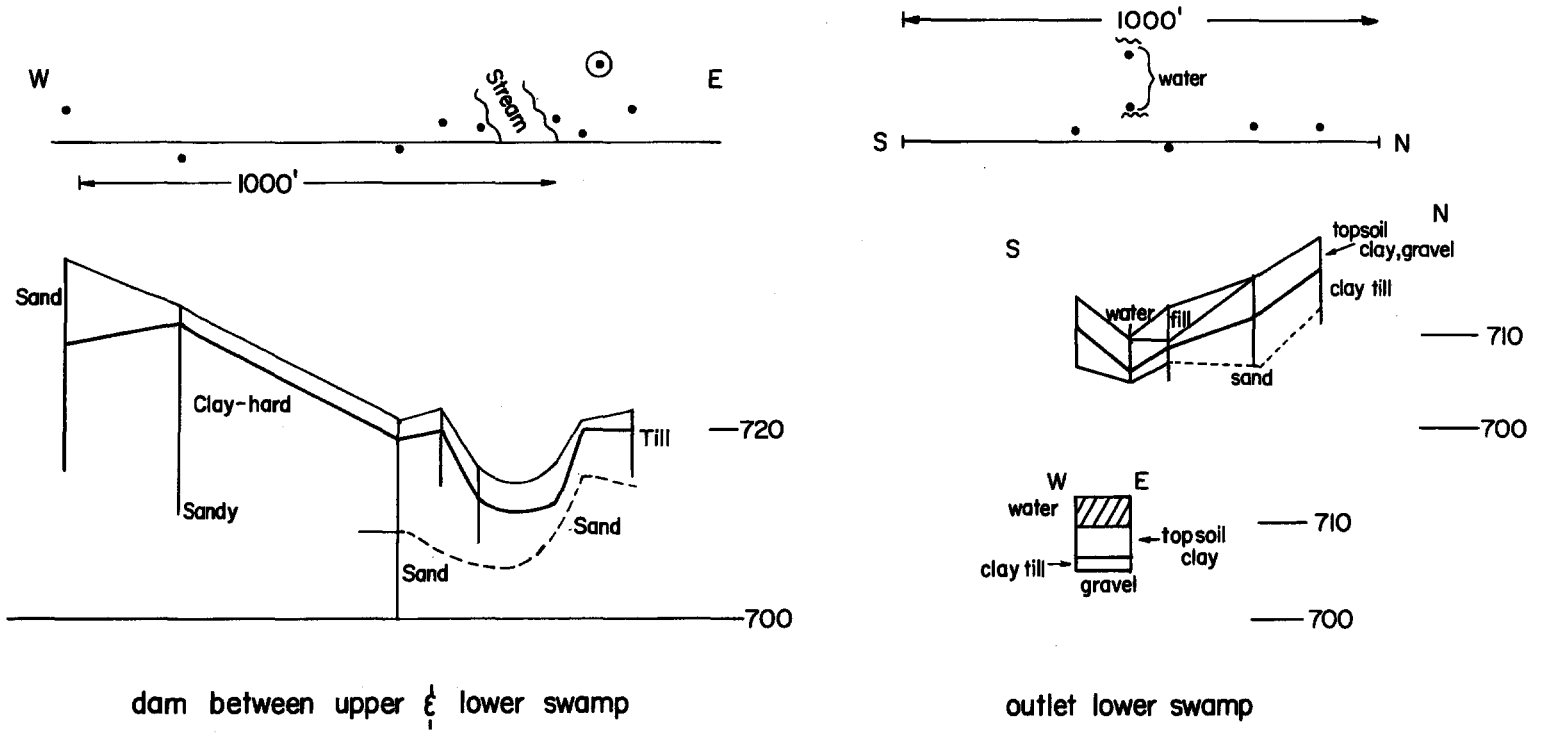

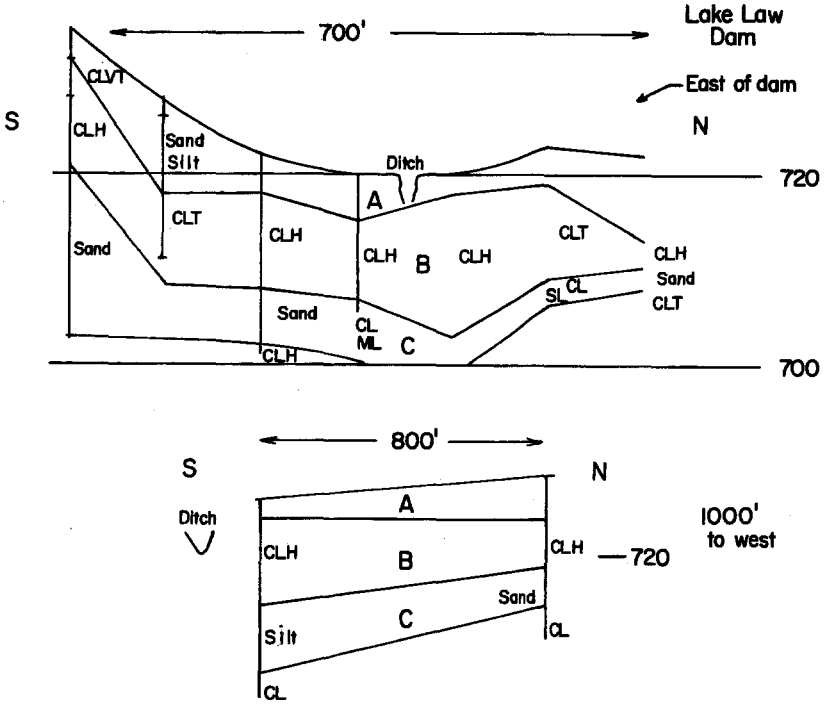

FIG. 7

Summary of limited subsurface information available - eastern side of POPAE.